Application of (super)cavitation for the recycling of process waters in paper producing industry

Janez Kosel, Matej Šuštaršič, Martin Petkovšek, Mojca Zupanc, Mija Sežun, Matevž Dular

PII: S1350-4177(19)31341-0
DOI: https://doi.org/10.1016/j.ultsonch.2020.105002
Reference: ULTSON 105002

To appear in: *Ultrasonics Sonochemistry*

Received Date: 26 August 2019
Revised Date: 3 February 2020
Accepted Date: 3 February 2020

Please cite this article as: J. Kosel, M. Šuštaršič, M. Petkovšek, M. Zupanc, M. Sežun, M. Dular, Application of (super)cavitation for the recycling of process waters in paper producing industry, *Ultrasonics Sonochemistry* (2020), doi: https://doi.org/10.1016/j.ultsonch.2020.105002

Application of (super)cavitation for the recycling of process waters in paper producing industry

Janez Kosel[a], Matej Šuštaršič[b], Martin Petkovšek[c], Mojca Zupanc[c], Mija Sežun[d], Matevž Dular[c]

[a]Institute for the Protection of Cultural Heritage of Slovenia;

[b]Eurofins ERICO Slovenija d.o.o.

[c]Faculty of Mechanical Engineering, University of Ljubljana, Slovenia

[d]Pulp and Paper Institute of Ljubljana, Slovenia;

Corresponding author: Dr Janez Kosel, email: janez.kosel@zvkds.si

Address: Poljanska 40, SI-1000, Ljubljana

Abstract

In paper production industry, microbial contaminations of process waters are common and can cause damage to paper products and equipment as well as the occurrence of pathogens in the end products. Chlorine omission has led to the usage of costly reagents and products of lower mechanical quality. In this study, we have tested a rotation generator equipped with two sets of rotor and stator assemblies to generate developed cavitation (unsteady cloud shedding with pressure pulsations) or supercavitation (a steady cavity in chocked cavitation conditions) for the destruction of a persistent bacteria *Bacillus subtilis.* Our results showed that only supercavitation was effective and was further employed for the treatment of waters isolated from an enclosed water recycle system in a paper producing plant. The water quality was monitored and assessed according to the chemical (COD, redox potential and dissolved oxygen), physical (settleable solids, insolubles and colour intensity) and biological methods (yeasts, aerobic and anaerobic bacteria, bacterial spores and moulds). After one hour of treatment, a strong 4 logs reduction was achieved for the anaerobic sulphate reducing bacteria and for the yeasts; a 3 logs reduction for the aerobic bacteria; and a 1.3 logs reduction for the heat resistant bacterial spores. A 22 % reduction in COD and an increase in the redox potential (37 %) were observed. Sediments were reduced by 50 % and the insoluble particles by 67 %. For bacterial destruction in real industrial process waters, the rotation generator of supercavitation spent 4 times less electrical energy in comparison to the previously published cavitation treatments inside the Venturi constriction design.

Keywords:

Rotational cavitation generator, hydrodynamic cavitation, paper mill industry, *Bacillus subtilis*, anaerobic sulphate reducing bacteria, COD, redox potential

1. Introduction

Water is essential for the paper producing process, because it permits the fibres to be transported from the apparatus which de-fibres the wood-pulp down to the manufacturing wire of the sheet of paper [1]. However, the continuously recycled process water (white water) contains organic substrates (starch), has favourable temperatures and a neutral pH, which is all in all an optimal environment for microbial growth [2]. Additionally, the development of bacteria gives rise to the accumulation of slime, which causes holes and spots or even breakage of the continuous paper sheet leading to expensive delays [3]. For disinfection purposes, chlorine is most commonly applied, however chlorination has several shortcomings among them the formation of carcinogenic organochlorines and the need for careful control of chlorine dosing [4,5]. Consequently, the Directorate-General for the Environment [6] issued guidelines for the elimination of all chemical molecules containing chlorine atoms in any form to produce cellulose bleached without chlorine- and chlorine derivatives (TCF or Totally Chlorine Free) and to label these products as ecologically friendly (Ecolabel flower; www.ecolabel.eu). However, the pulp that fulfils these standards has lower mechanical properties, requires larger quantities of wood and uses costly reagents, such as ozone. Therefore, alternative methods are being developed that are safe, easy to perform, inexpensive, less labour intensive but effective, and hydrodynamic cavitation is one of such options [7].

Cavitation is a physical phenomenon caused by the formation of vapour bubbles in an initially homogeneous liquid due to the decrease of local pressure at an approximately constant temperature [8]. It is composed of various physical (pressure pulses, shear forces, high local temperatures) and chemical side effects (decomposition of H_2O mainly to $^{\bullet}OH$ and other radicals). Ultrasonic

cavitation has been proven to be efficient for the intensification of oxidation reactions (H_2O_2 and $^{\bullet}OH$) [9,10] and for the destruction of bacteria [11–13]. It provides significantly higher rates for the Weissler reaction (oxidation of iodide to iodine by the cavitation produced H_2O_2) in comparison to the hydrodynamic cavitation [14]. In specific energy terms, hydrodynamic cavitation has a maximum efficiency of about 5 x 10^{-11} moles of tri-iodide/joule of energy compared with the maximum of almost 8 x 10^{-11} moles of tri-iodide/joule for ultrasonic cavitation [15]. Consequently, ultrasonic cavitation has been successfully applied in various industrial applications [16–19]. These include the synthesis of nanomaterials [16], the generation of highly viscoelastic micelles [20] and the disinfection of wastewater [17]. However, hydrodynamic cavitation can treat larger volumes for a similar energy input and can be easily adopted for large scale continuous flow-through industrial applications with significantly lower equipment costs [21]. Therefore, even though hydrodynamic cavitation produces a lesser amount of reactive oxygen species it is still more efficient considering the relative energy input and the scale of operation [22].

Hydrodynamic cavitation forms due to relative velocity increase between the liquid and the submerged body. Cavitation bubbles form, when the local velocity increases and causes static pressure to drop below the critical vaporization pressure. Most common hydrodynamic cavitation can be seen on hydraulic turbine machinery on rotor's blades passing through the liquid [23,24] or behind the constrictions, where liquid is forced to pass through [25].

Several types of hydrodynamic cavitation can form; specifically, for the present setup, we could observe developed unsteady cavitation and supercavitation. Developed unsteady cavitation is formed when cavitation clouds start to shed thus creating pressure pulsations, vibration, erosion,

high local temperatures and noise, and can be used for the destruction of bacteria [26,27]. When system pressure is decreased or when flow velocity is increased a small cavity will grow and a large single steady vapour filled supercavity will develop [8], for which larger disturbances in pressure and temperature are uncommon (noise, vibration and erosion are absent). Therefore, it can be expected that supercavitation does not cause any significant physical damage to microbial cells. Nonetheless, Šarc et al. [28] observed that supercavitation generated inside the Venturi constriction was effective for the disinfection of the pathogenic bacteria *Legionella pneumophila* in tap water, while developed unsteady cavitation removed only 28 % of the viable count. They proposed that the disinfection mechanism could be attributed to the rapid pressure change between the entrance and exit of the supercavitation cavity. Similarly, Gottlieb et al [29] proposed that a mixture of effects such as instant pressure decrease –pressure shock at the entrance point of the supercavity (transition from the liquid/vapour phase) and instant pressure increase (at the closure of supercavity) play a role in the rupture of bacterial wall.

Our aim was to assess the applicability of the rotation generator of hydrodynamic cavitation (RGHC) [30] for the treatment of process waters from a paper producing plant. For this purpose, the starting cavitation experiments were performed on tap water spiked with a Gram-positive bacteria *Bacillus subtilis.* This sporogenic, biofilm forming bacteria was selected because it has a thicker peptidoglycan cell wall (in comparison to Gram-negative bacteria which have a much thinner peptidoglycan layer) and is thus more resistant to mechanical stresses [31], is persistent in paper industry as it can hydrolyse fibre-bound galactoglucomannans from soft-wood pulp to produce simple sugars [32], can spoil surface sizing materials of paper making [33], and can survive high temperature treatments in paper mills [34]. To examine the effect of both developed

unsteady cavitation and supercavitation, two sets of specifically designed rotors and stators were produced for the RGHC machine and were tested on spiked tap water preparations. Finally, to verify our RGHC device, we sampled real process waters from an enclosed recycling system of a paper producing plant and after cavitation treatments the survivability of the major classes of microorganisms and the chemical and physical changes of samples were assessed.

2. Methods

2.1 Hydrodynamic cavitation set-up

In this study, the effects of cavitation on different microorganisms problematic for paper mill industry were investigated using a rotational generator of hydrodynamic cavitation (RGHC) which was first described by Petkovšek et al. [30]. The RGHC is based on the centrifugal pump design which has a modified rotor and a stator added in its housing (Figure 1). The RGHC is powered by an electric motor of 500 W that propels the modified rotor. Maximum rotational frequency of the electric motor is 10,000 revolutions per minute (rpm). The stator's position is opposite to the rotor (both 50 mm in diameter; r = 25 mm) and the housed unit of rotor and stator forms the so-called cavitation treatment chamber. The RGHC preserves its flow-through pumping function, which makes its installation into the water pipe system simple with no additional pumping required. In our experimental setup, the RGHC was placed in a closed loop experimental water system which is presented in Figure 2. The experimental setup is made of piping which connects a 2 L reservoir, a heat exchanger, pressure and flow meters and the RGHC device. The piping and connections are made of standard household water system materials [35].

Two different rotor and stator designs were used in order to generate developed cavitation and supercavitation (Fig. 1). The rotor and stator pair used for developed cavitation have a specially designed surface geometry with 12 radial teeth, 3 mm deep and 4 mm wide. The area of each tooth of this serrated rotor disc has been designed in a way that its surface is angled at 8°, giving it a sharp leading edge. When aligned, the space between the angled surface of the individual rotor's tooth and the completely flat surface of the individual stator's tooth resembles the Venturi nozzle geometry (Fig. 3A).

In the case of supercavitation set-up, an additional flow regulation valve was installed at the inlet of the RGHC (Fig. 2B) to manipulate the pressure inside the treatment chamber. By closing the valve, the flow rate through the RGHC gets severely reduced. The surface geometry of the rotor used for supercavitation consists of two symmetrical teeth (hence its name the two teeth rotor), which resembles the symmetrical Venturi design, first described by Zupanc et al. [36] (Fig. 3C). The divergence angle of the teeth's cross section is 10° and the secondary divergence angle is 30° (Fig. 3B). The surface of the added stator is completely flat and has no teeth with the aim not to induce any additional pressure fluctuations (this allows for the development of a large steady supercavity behind each rotor's tooth). When using the rotor-stator configuration for supercavitation the electric motor is able to achieve the maximum rotary frequency (10,000 rpms), while in the case of rotor-stator configuration with grooves for developed cavitation, the rotary frequency is reduced to 9,000 rpms due to motor's power limitations.

For both the serrated rotor and the two teeth rotor, the gaps between the rotor and the stator were set to be 1 mm (gap length; l). When in motion, the rotor's teeth force the liquid to move in a radial direction - causing centrifugal forces, which result in a pumping function of the RGHC. The high

frequency of rotation also causes the movement of liquid in the tangential direction. The narrow gap between the rotor and the stator and sharp edges cause high shear stress and consequently intense pressure pulsations resulting in cavitation formation (Fig.3). In the case of the two teeth rotor there is enough space between the teeth so that a large and stable cavitation cavity forms behind each tooth, which resembles a supercavitation cavity (Fig. 3B). Each entire flow of the 2 L sample through the treatment chamber is defined as one cavitation pass.

Both rotors were made of stainless steel and both stators were made of a transparent acrylic glass and these also functioned as a cover. Both materials used are inert and don't allow for any chemical reactions between the sample liquid and the machine.

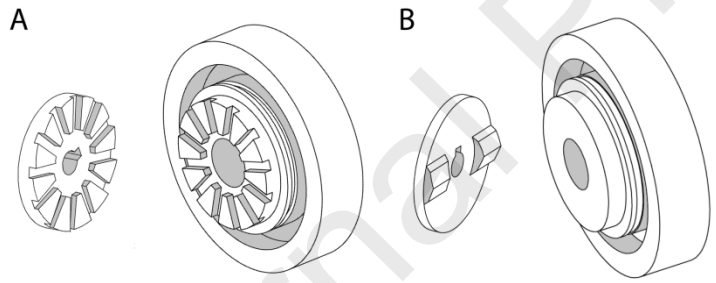

Fig. 1: Rotor-stator design for developed cavitation (left) and supercavitation (right).

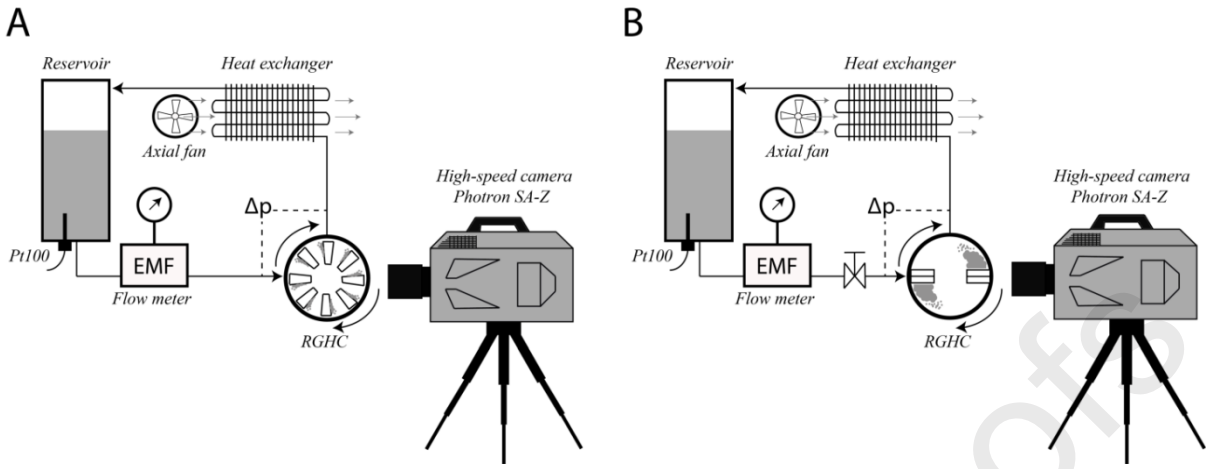

Fig. 2: Experimental setup scheme for the developed cavitation (A) and supercavitation (B).

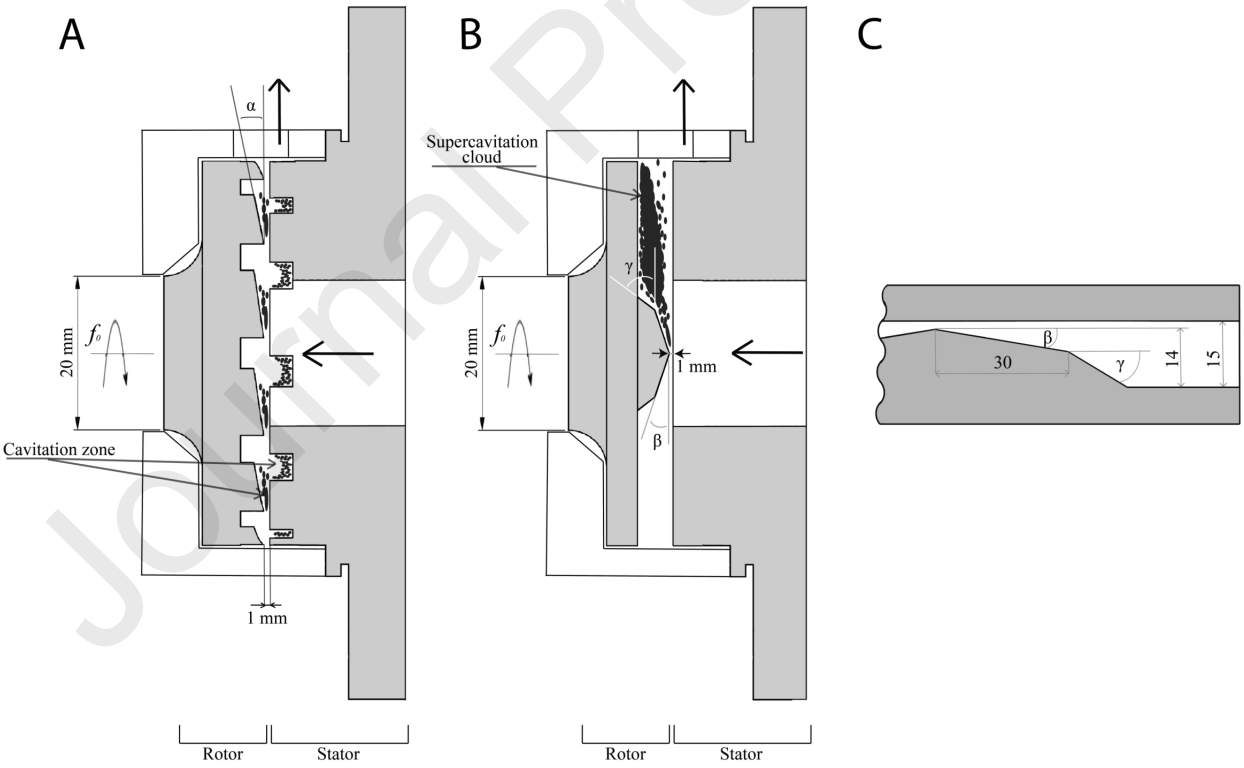

Fig. 3: Scheme of the treatment chamber of the rotation generator. The rotor and stator pairs used for developed cavitation and supercavitation are presented under A and B, respectively. Both rotors are rotating in a counter clockwise fashion where water is entering in the axial direction through the stator before exiting in the radial direction. Under C the geometry of a Venturi constriction is presented. Angles are indicated by α (8°), β (10°) and γ (30°).

Measurements of the local system pressure (P_L), were conducted upstream of the treatment chamber (on the suction side) using the Hygrosens DRTRAL-10 V-R16B pressure probe (uncertainty of ± 0.2%). The flow rate was measured using the Buerkert SE32 flow meter (uncertainty of ± 1%). Sample temperature was monitored by a resistance temperature sensor Pt100 (uncertainty of ± 0.2 K), installed directly into the reservoir. In the experimental setup the installed heat exchanger was cooled by an external fan with ambient air, preventing any heating of the treated sample above 30 °C. The stator was made of transparent acrylic glass due to visualization and functioned as a cover. High-speed visualization was performed using Photron SA-Z, which enables recording with 20,000 frames per seconds at full resolution (1024 x 1024 pixels) and can go up to 2.100,000 fps at reduced resolution. For the present case visualization was performed with 75,000 fps at resolution of 512 x 465 pixels. The illumination was performed with high intensity LED, focused into the observed area from the same direction, but with a slight angle to the camera. The camera was focused perpendicularly to the rotor's teeth in axial direction of the rotor. The motor's power and energy consumption were monitored with a Power Analyzer Norma 4000.

2.2 Microbiological measurements

2.2.1. Working suspension preparation

B. subtilis ATCC® 6633™ acquired from the Veterinary Faculty at the University of Ljubljana was cultured at 37 °C on standard count agar plates (*SCA,* Merck™; 3,0 g/L of meat extract, 5,0 g/L of peptone from casein, 5 g/L of sodium chloride, and 12 g/L of agar). For the hydrodynamic cavitation experiments colonies from fresh culture plates (24 h old) were harvested, suspended and diluted in sterile Ringer solution (Merck™) until a concentration of around 5 Log_{10} CFU mL^{-1} (high initial bacterial titer) or 2 Log_{10} CFU mL^{-1} (low initial bacterial titer) was achieved. Bacterial concentration was determined by optical density measurements at 650 nm (OD_{650}). The prepared suspension was then stored on ice in a Styrofoam box and just before the cavitation run, the bacterial culture was further diluted 100 and 10,000 times to a final working concentration of around 1.0 x 10^5 CFU mL^{-1} (high initial titer) and of around 1.0 x 10^2 CFU mL^{-1} (low initial titer). The sample volume for the rotation generator was 2 L.

2.2.2. Sampling and quantification

Apart from the experiments with the *B. subtilis* working suspension, 5 L samples were also taken from real technological process waters isolated from a board paper mill plant. These samples were collected from the individual pool (recycled water or RW) or from the central pool (central recycled water or CRW) of an enclosed water recycle system and were analysed for the presence of anaerobic sulphate reducing bacteria, aerobic bacteria, bacterial spores as well as for yeasts and moulds (Figure 4). The original pH value of RW and CRW samples was 7.6. All samples were kept refrigerated (4 °C) until analysis.

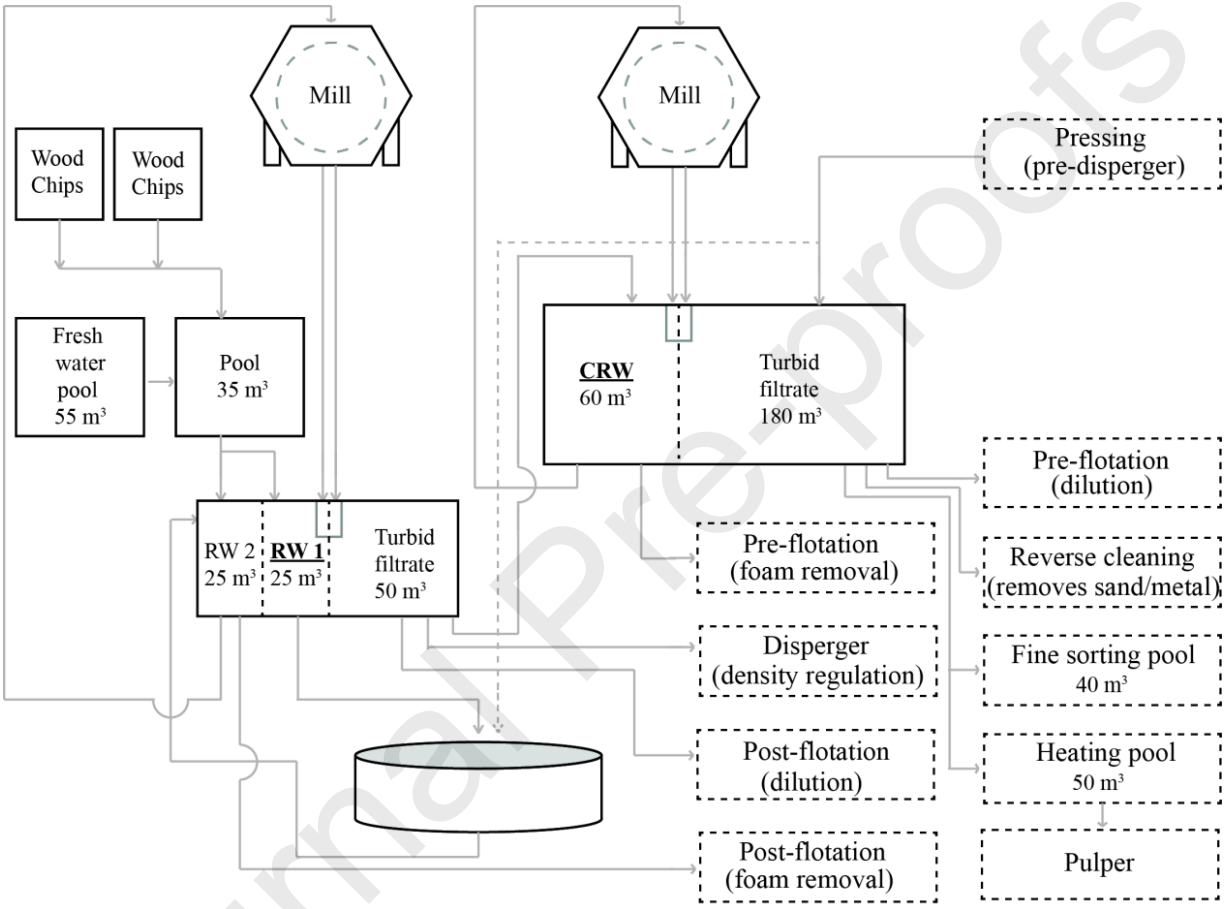

Fig. 4: The schematic presentation of the production section in the board paper mill plant Vipap Videm Krško from which 5 L samples were taken. The first sample was collected from the individual pool (RW1 = RW) and the second sample from the central pool (CRW) of an enclosed water recycle system. The places of sampling on the scheme are presented in bold and are underlined.

Before each experiment, 2 L of sample were introduced into the feeding reservoir and then cavitated for a predetermined time (30 and 60 min for both developed cavitation and supercavitation). The samples for analysis were taken prior, during and after the experiments, and for each sample 40 ml of suspension were released from the device through the sampling valve and poured back into the cavitation device through the entry valve. This ensured that the trapped dead volume inside the sampling pipe (that was not cycled through the cavitation device) was not analysed. Then the next 10 mL were released for the same sampling pipe and were stored in 50 mL tubes on ice in a Styrofoam box.

The impact of hydrodynamic cavitation on the destruction of bacteria *B. subtilis* was monitored by colony counts. For this, samples of 1 mL were plated on the SCA agar medium using the 10-fold successive dilution method in saline solution. Colonies were counted after a 48 h long incubation period at 37 °C and results were expressed in Log_{10} CFU mL^{-1}. For the selective isolation and quantification of yeasts from RW and CRW samples, 1 mL was plated on the Sabouraud Dextrose Agar plates (SDA, Merck™, 10 g/L of peptone, 40 g/L of dextrose, 2.0 % agar) and colonies were counted after a 7 days long aerobic incubation at 28 °C. For the quantification of aerobic bacteria from RW and CRW samples, 1 mL was plated on SCA Petri plates and colonies were counted after 48 hours at 37 °C. The bacterial spore count was performed in the same manner as for the aerobic bacteria with the exception of additional thermal pre-treatment of samples (80 °C for 20 min) before plating on solid SCA plates. The thermal shock destroys the vegetative portion of cells and only spores survive. Mould colony counts for the RW and CRW samples were performed by adding 1 mL of sample into a screw-cap tube (20 × 150 mm) containing 30 mL of freshly autoclaved, still molten (at 50 °C in a water bath) SDA agar medium. The content was vortexed, poured into a Petri plate and incubated at 25 °C for 5 days [37]. Quantification of the anaerobic

sulphate reducing bacteria in these two real water samples differed from the standard colony counting technique. Firstly, 5-fold serial dilutions were prepared and 1 mL of each dilution was poured into a screw-cap tube (20 × 150 mm) containing 10 mL of freshly autoclaved, still molten (at 50 °C in a water bath), iron-sulphite agar medium (Merk™, 10 g/L of pancreatic digest of casein, 1 g/L of Na_2SO_3, 0.1 g/L of iron powder and 2 % agar). During anaerobic incubation, the tubes were almost completely filled with media and were tightly sealed with screw caps. Additionally, the iron inside the media combined with any dissolved oxygen and thus provided an anaerobic environment. The strongest serial dilution that still proved positive (black colouration) after a 7 days long incubation at 37 °C was determined as the concentration of sulphate reducing bacteria and was presented in Log_{10} CFU mL^{-1} according to its logarithmic order of dilution. All values reported in this paper are the mean of at least two independent biological treatments and three replicates for each treatment. The average values and standard deviations are given.

To evaluate the impact of cavitation on the overall growth reduction, a specific decay rate constant (μ) was calculated as follows:

$$\mu = \frac{\ln X_f - \ln X_0}{t_f - t_0}. \quad (1)$$

Specific decay rate (1/h) is the slope of the microbial growth curve and is negative when cells start dying [38]. X_0 is colony count per millilitre at the beginning of treatment; X_f is colony count per millilitre at the end of treatment; t_0 is time at the beginning of treatment and t_f is time at the end of treatment.

To ensure that the hydrodynamic device was free of microorganisms, before and after each hydrodynamic cavitation experiment, the device was cleaned using a washing protocol. This

consisted of one rinse with tap water (running the hydrodynamic cavitation device filled with tap water for 5 min), two 15 min long rinses with 0.5 % organic peroxide (peracetic acid, Persan® S15, Belinka Perkemija, d.o.o., Slovenia), and finally six successive device volume rinses with tap water (each lasting 5 min). The rinsed water was disposed after an overnight exposure to active chlorine. To determine the effectiveness of washing between cavitation experiments, the tap water from the last rinse was sampled and quantified by colony counts. Additionally, before each cavitation run, the effect of possible bacterial attachment on the interior surfaces of the cavitation reactor was tested. For this purpose, samples were taken immediately before (sampled directly form the flask containing the prepared bacterial suspension) and after filling the reactors with tap water containing around 5 Log_{10} CFU mL^{-1} or 2 Log_{10} CFU mL^{-1} of bacteria *B. subtilis*, and colony counts were compared. If compared values were similar (before and after filling), no significant bacterial attachment was present.

2.3 Physicochemical analysis

Organic matter (chemical oxygen demand, COD), was measured using COD kits (Hach Lange LCK 314 for samples with a COD value between 15 mgO_2/L - 150 mgO_2/L and LCK 714 for samples with a COD value between 100 mgO_2/L - 600 mgO_2/L) and a spectrophotometer DR3900 Hach Lange. pH value, redox potential and dissolved oxygen level were determined during sampling on site, using a Multi 340i analyser (WTW, Germany). Redox potential values (Pt electrode) measured in the field with an Ag/AgCl reference electrode were normalized to 25 °C and referenced to the standard hydrogen electrode (Eh). Settleable solids were analysed according to the Deutsches Institut fur Normung DIN 38409-2 [39], in which settleable substances were shaken and timed sedimentation was determined in a measuring container. Insolubles were

determined according to SIST ISO 11923 [40], for which Sartorius Glass-Microfibre Discs GMF3 filter paper was used for filtration. After drying the filter at 105 °C, the weight of the residual mass on the filter was measured. Colour intensity measurements were carried out in terms of the spectral absorption coefficient (SAC) using absorbance measurements at three wavelengths (436 nm, 525 nm and 620 nm) by UV-visible absorption with a Varian Cary 50 UV-Vis spectrophotometer (1 cm cell width, Agilent) after the samples were filtered using a 0.45 μm filter in accordance with the ISO 7887 [41]. In this way, SAC values were calculated according to the below equation:

$$SAC(m^{-1}) = \frac{100 \times Abs(\lambda)}{d}, \quad (2)$$

where *Abs(λ)* is the absorbance at a given wavelength (*λ*), and *d* represents the measuring cell width (mm).

3. Results

3.1 Hydrodynamic cavitation development

To visualise the cavitation development inside the treatment chamber a series of image sequences were recorded using a high-speed camera Photron SA-Z (Fig. 5). The sequences follow a series of five 0.4 ms long intervals. The rotor was rotating in a counter clockwise fashion.

In order to generate developed unsteady cavitation, the RGHC was equipped with the serrated rotor (and stator; r_{rotor} of 0.025 m) which was spun at 9,000 rpm with a tangential speed of fluid reaching 23.6 m/s. The entire set-up presented in figure 2 A had a flow rate of 1.8 L/min (Table 1). According to our high-speed camera measurements performed in this study, a strong form of developed cavitation was visible behind every gap between the tips of the teeth of the opposing rotor and stator. Violent shedding and bubble collapsing were observed (Figure 5 B).

In order to generate supercavitation the RGHC was equipped with the two-teeth rotor (r_{rotor} of 0.025 m) which was spun at around 10,000 rpm with a tangential speed of fluid reaching 26.0 m/s. Because

of the chocked cavitation conditions (generated using an added valve installed at the inlet of the RGHC) the entire set-up presented in figure 2 B had a flow rate of only 0.2 L/min. Filming with the high speed camera revealed the formation of a large and stable vapour cavity which filled most of the volume behind every tip of both teeth (Figure 5D). In detail, two specific features of cavitation were formed on the presented supercavitation rotor. Cavitation cavity at the outer parts of the rotor resembled a unified supercavity. The second feature comprised of cavitation shedding that was caused because fluid velocity was dropping towards the centre of the rotor. For the purposes of clarity, we will be using the term supercavitation to describe the simultaneous formation of the unified supercavity and the shedding part of cavitation.

Table 1: Operational characteristics of the rotation generator.

RGHC operation	**Rotor type**	**Flow rate (L/min)**	**Revolutions of rotor (rpm)**	P_L **(kPa)**
Developed unsteady cavitation	*Serrated rotor*	1.8	9,000	117.2
Supercavitation	*Two-teeth rotor*	0.2	10,000	93.3

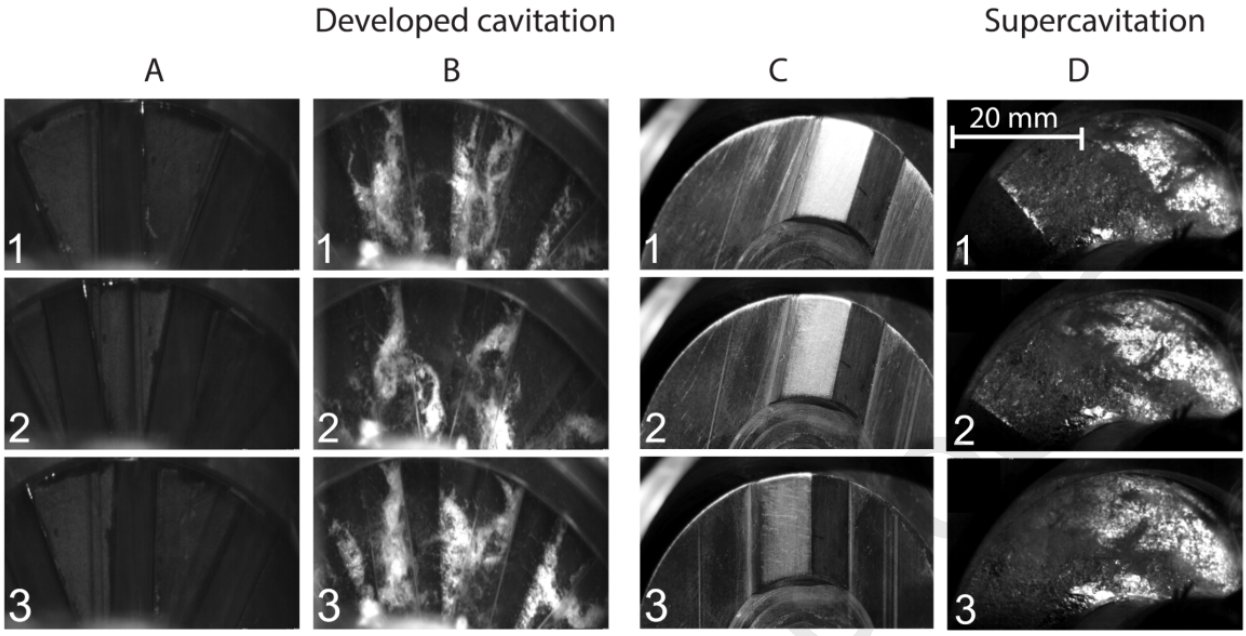

Fig. 5: Hydrodynamic characteristic of the rotation generator equipped with the serrated rotor (A) (for developed cavitation) and the two teeth rotor (C) (for supercavitation). Developed cavitation can be observed under column B and supercavitation under column D.

3.2 Validation of cleaning and bacterial attachment

The washing protocol employed for the RGHC device successfully removed all *B. subtilis* presence between different cavitation experiments. Additionally, we found that colony counts of *B. subtilis* samples that were taken immediately before and after the filling of the RGHC device (with the *B. subtilis* suspension) differed only slightly (a maximum difference of 0.15 $\log_{10}$ CFU mL^{-1}).

3.3 Hydrodynamic cavitation for the destruction of B. subtilis

The effect of hydrodynamic cavitation generated inside the RGHC on the destruction of bacteria *B. subtilis* is presented in Figure 6. In these experiments, the samples were exposed to cavitation for 60 min, which relates to 54 cavitation passes for developed cavitation and to 6 cavitation passes for supercavitation (as described in Šarc et al. [42]).

When the RGHC device was equipped with the serrated rotor for the formation of multiple zones of developed cavitation, the viable count of the high initial bacterial titer (5.0 Log_{10} CFU mL^{-1}) remained relatively unaffected for the first 27 passes through the treatment zone. After that, the viable count decreased slowly until the end of the experiment when the count was reduced down to 4.6 Log_{10} CFU mL^{-1}. In all, a slight reduction of 0.4 logs was achieved after 54 cavitation passes. However, when the RGHC was equipped with the two-teeth rotor for the generation of supercavitation, the viable count of the high initial bacterial titer (5.4 Log_{10} CFU mL^{-1}) rapidly declined and after 6 supercavitation passes the count was reduced down to only 3.1 Log_{10} CFU mL^{-1}. In all, a staggering 2.3 logs reduction (a 99.50 % destruction) was achieved.

Similar trends were observed for low initial bacterial titers. When RGHC was spun with the serrated rotor, the low initial titer (2.6 Log_{10} CFU mL^{-1}) was slowly reduced to 2.3 Log_{10} CFU mL^{-1} after 54 cavitation passes. The total reduction of viable count was almost the same as that observed for the high initial titers. However, when supercavitation was generated (two-teeth rotor), the low initial titer count (2.8 Log_{10} CFU mL^{-1}) was again strongly reduced and after 6 supercavitation passes only 1.6 log_{10} CFU mL^{-1} remained viable.

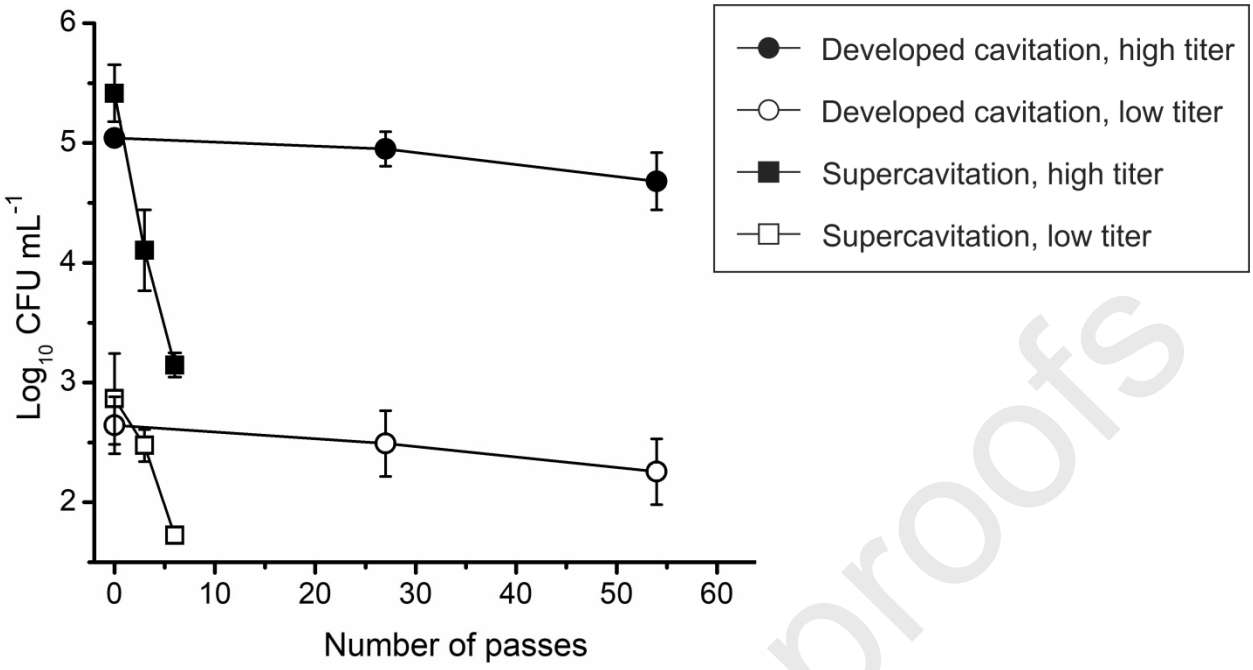

Fig. 6: The Influence of developed cavitation (serrated rotor; circles) or supercavitation (two-teeth rotor; squares) generated inside the RGHC device on the destruction of high (filled symbols) or low (empty symbols) spiked titers of the bacteria *Bacillus subtilis*.

3.4 Supercavitation for the recycling of real process waters

The effects of supercavitation (RGHC equipped with the two-teeth rotor), on the destruction of the major classes of microorganisms which were found to be present in the RW and CRW samples and on the chemical and physical characteristics of these samples are presented in Figures 7, 8 and 9. The RW or CRW samples were exposed to cavitation for 60 min, which relates to 6 supercavitation passes.

After 6 supercavitation passes, the COD for the RW and CRW samples was reduced by 22 %, and by 10 %, respectively (Figure 7). However, the redox potential was increased by cavitation. Specifically, the increase in the redox potential was much stronger for the CRW samples (77 %)

than for the RW samples (37 %) reaching 160 mV and 107 mV, respectively. Supercavitation treatment increased the content of dissolved oxygen from 5.3 mgO_2/L to 7.3 mgO_2/L for the RW samples and from 4.6 mgO_2/L to 7.4 mgO_2/L for the CRW samples.

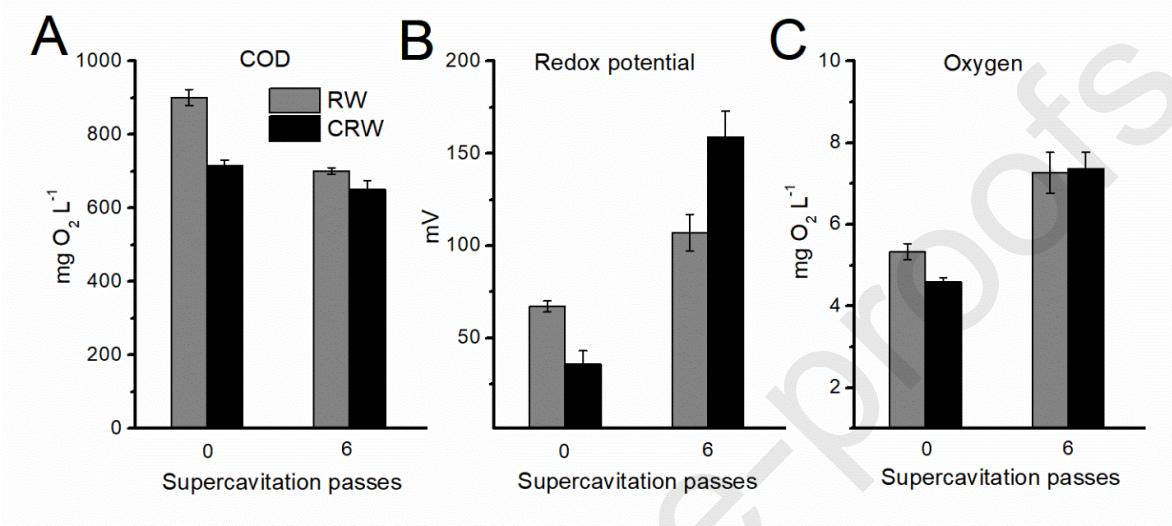

Fig. 7: The effect of the RGHC supercavitation treatment (two-teeth rotor) on the chemical parameters of samples isolated from real process waters.

After supercavitation the level of sediments was reduced by 50 % and by 95 % for the RW and CRW samples, respectively (Figure 8). Similar results were obtained for the insoluble materials of the RW and CRW samples for which a 67 % and a 48 % reduction was achieved. Contrary to this, the SAC values increased for both sample types. The SAC_{436}, SAC_{525}, and the SAC_{620} values (m^{-1}) increased by 96 %, 93 % and by 97 % for the RW samples and by 43 %, 28 % and by 63 % for the CRW samples, respectively.

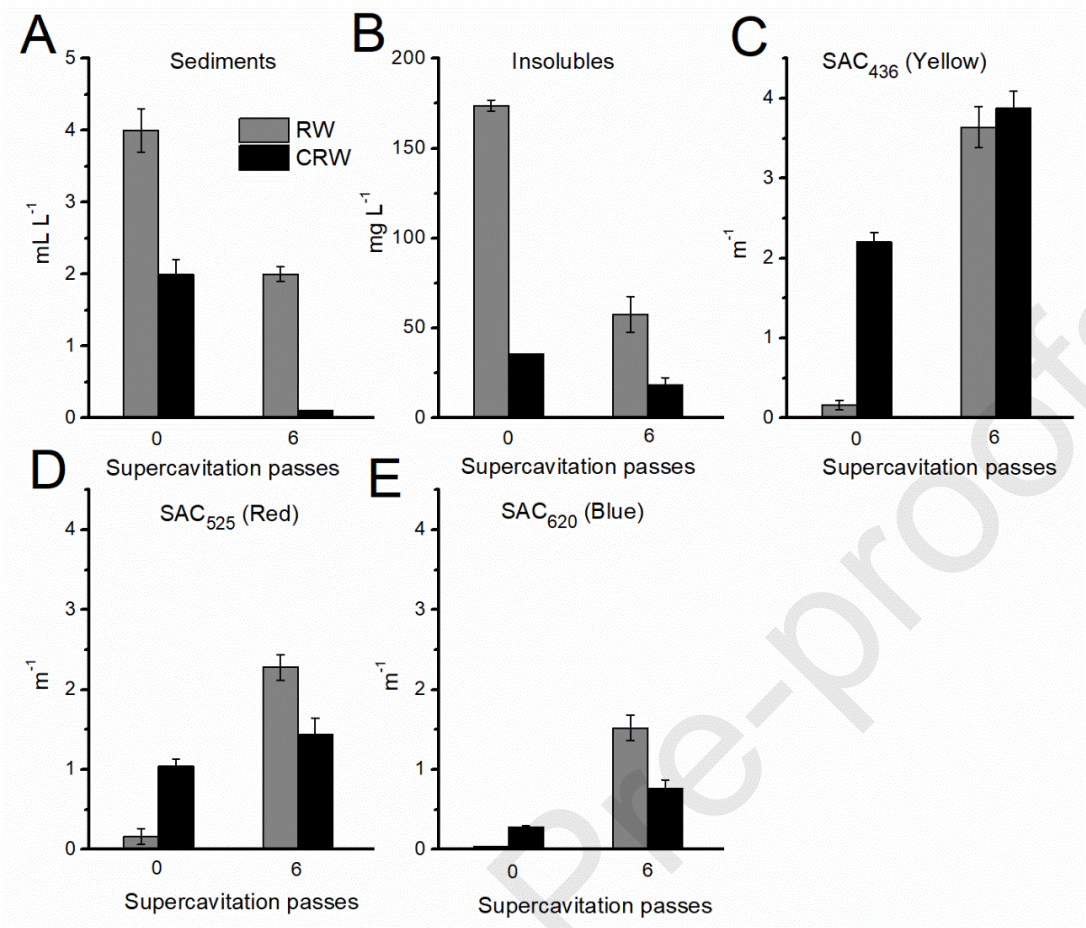

Fig. 8: The effect of the RGHC supercavitation treatment (two-teeth rotor) on the physical parameters of samples isolated from real process waters.

Supercavitation treatment strongly reduced the viable count of all the major classes of microorganisms which were found to be present in the RW and CRW samples. During the cavitation treatment the viable count of aerobic bacteria in the RW sample was reduced from 5.9 Log_{10} CFU mL^{-1} to 3.2 Log_{10} CFU mL^{-1}. Therefore, a staggering 2.7 logs reduction was achieved after 6 supercavitation passes (a 99.81 % destruction). However, for the CRW samples the reduction of the aerobic bacterial count was smaller (1.2 logs reduction). A 4.2 logs (a 99.99 % destruction) and 2.8 logs (a 99.84 % destruction) strong reduction of the anaerobic sulphate reducing bacteria was observed for the RW and the CRW samples, respectively. Viable yeast count

reduction was also strong, again reaching 4 logs (a 99.99 % destruction) and 2.5 logs (a 99.72 % destruction) for the RW and CRW samples, respectively. Viability of bacterial spores was reduced from 2.6 Log_{10} CFU mL^{-1} to 1.3 Log_{10} CFU mL^{-1} for the RW samples and from 2.8 Log_{10} CFU mL^{-1} to 1.0 Log_{10} CFU mL^{-1} for the CRW samples. Finally, although present at lower concentrations, moulds were reduced by 0.6 Log_{10} CFU mL^{-1} and by 0.3 Log_{10} CFU mL^{-1} for the RW and CRW samples, respectively.

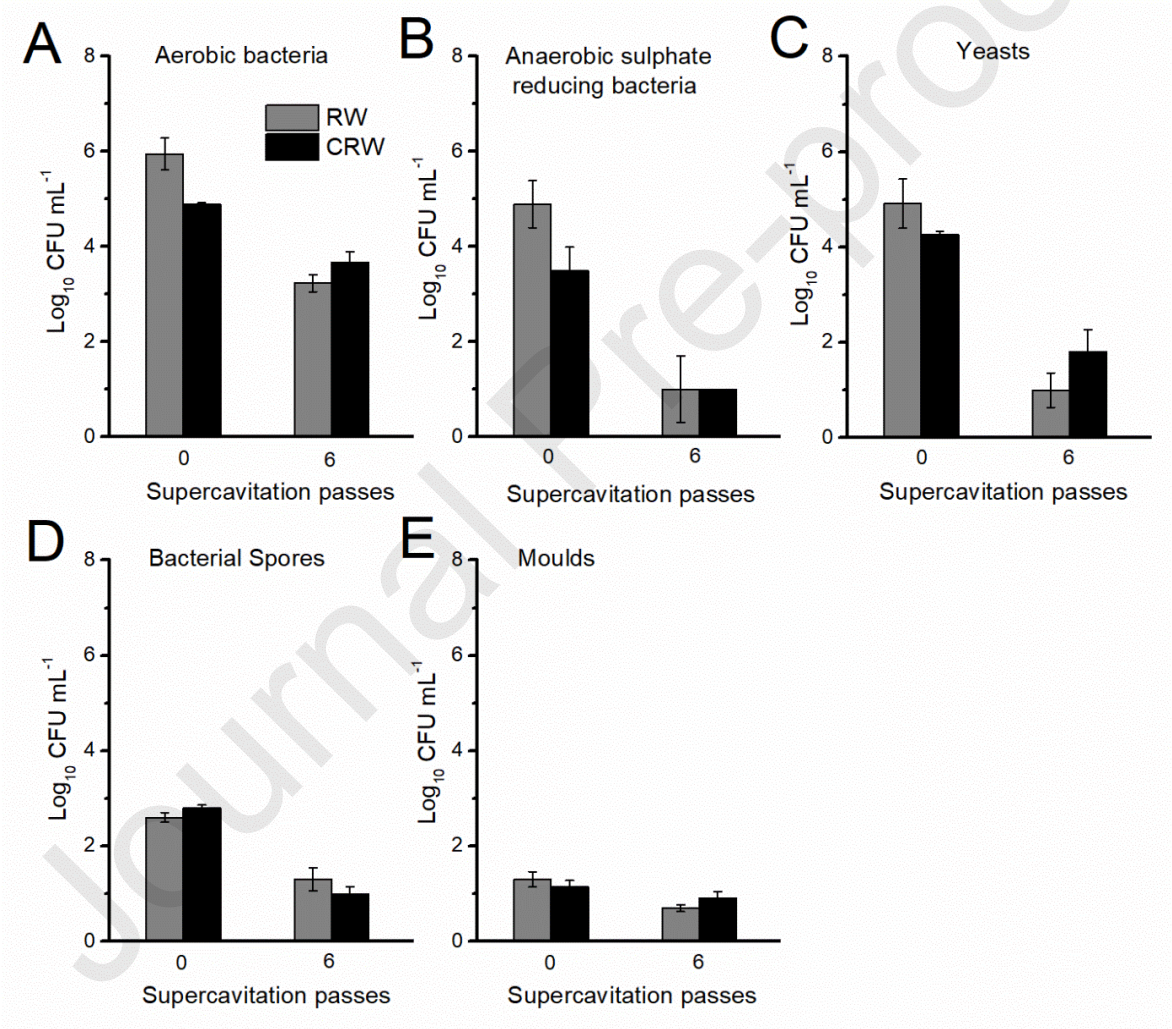

Fig. 9: The effect of the RGHC supercavitation treatment (two-teeth rotor) on the destruction of the major classes of microorganisms which were present in real process waters.

3.5 Economic evaluation

Operational effectiveness of the RGHC equipped with the serrated (for developed unsteady cavitation) or the two-teeth rotor (for supercavitation) was compared with the effectiveness of the Venturi device, which was assembled by Arrojo et al. [43] and which could generate a developed form of cavitation. For both devices, electric energy per order (E_{EO}; kWh/m^3/order) was calculated [44], which is the amount of electric energy required to bring a decrease in viable colony counts (CFU/mL) by one order of magnitude. Its equation is presented below:

$$E_{EO} = \frac{P \times t_f}{V \times Log_{10}(\frac{X_0}{X_f})}, \quad (3)$$

where P is the power input of the system [kW], V is the volume of treated water [m^3] in time t [h], and X_0 and X_f are the starting and ending viable colony counts of bacteria per one millilitre (CFU/mL). Higher E_{EO} values correspond to lower removal efficiencies. Table 2 shows the average E_{EO} values and approximate costs (€/m^3) for each experimental run. Nevertheless, we have to keep in mind that these costs only relate to electric energy consumption of each individual run and do not include any potential cooling costs, and capital or maintenance costs are also excluded (plant production, amortization and operation).

The E_{EO} value for the removal of the bacteria *Escherichia coli* (with a starting concentration of 1 x10^4 CFU mL^{-1}) from wastewater using the Venturi device was 268.6 kWh/m^3/order [43]. For a similar starting bacterial titer (~1 x 10^5 CFU mL^{-1}) of *B. subtilis,* the RGHC spent 347.5 kWh/m^3/order and 67.2 kWh/m^3/order for the developed cavitation and for the supercavitation, respectively. When the RW sample was treated using supercavitation, the RGHC spent 56.2, 36.4,

39.0, 117.4 and 253.5 kWh/m^3/order for the aerobic bacteria, anaerobic sulphate reducing bacteria, yeasts, bacterial spores and for moulds, respectively.

Table 2: Electrical efficiency of the rotation generator equipped with the serrated (for developed unsteady cavitation) or the two-teeth rotor (for supercavitation) in comparison to the Venturi device assembled by Arrojo et al. [43].

Device	**Cavitation development**	**Bacterial species**	t_f **(h)**	***TMP*** **(kW)**	V **(m^3)**	X_0 **(CFU/mL)**	X_f **(CFU/mL)**	μ **(t_f - t_0) (1/h)**	E_{EO} **(kWh/m^3/order)**	***Cost*** **(€/m^3)**
Venturi #3	*Developed unsteady cavitation*	*Escherichia coli*	2[A]	5[A]	0.05[A]	$1{\cdot}10^{4}$[A]	$1.8{\cdot}10^{3}$[A]	-0.85[A]	268.6[A]	26.9[A]
RGHC Serrated rotor	*Developed unsteady cavitation*	*Bacillus subtilis*	1	0.250	0.002	$1.1{\cdot}10^{5}$	$4.8{\cdot}10^{4}$	-0.83	347.5	34.7
RGHC Two teeth rotor	*Supercavitation*	*Bacillus subtilis*	1	0.305	0.002	$2.6{\cdot}10^{5}$	$1.4{\cdot}10^{3}$	-5.22	67.2	6.7
		Aerobic bacteria (RW)	1	0.310	0.002	$8.9{\cdot}10^{5}$	$1.7{\cdot}10^{3}$	-6.26	56.2	5.6
		Anaerobic sulphate reducing bacteria (RW)	1	0.310	0.002	$7.8{\cdot}10^{4}$	5	-9.70	36.4	3.6
		Yeasts (RW)	1	0.310	0.002	$8.2{\cdot}10^{4}$	$1.0{\cdot}10^{1}$	-9.01	39.0	3.9
		Bacterial spores (RW)	1	0.310	0.002	$3.9{\cdot}10^{2}$	$2.0{\cdot}10^{1}$	-2.9	117.4	11.7
		Moulds (RW)	1	0.310	0.002	$2.0{\cdot}10^{1}$	5	-1.4	253.5	25.4

[A]Results obtained from Arrojo et al. [43].

4. Discussion

In this work, we studied 2 different types of hydrodynamic cavitation, developed unsteady cavitation (using a serrated rotor and stator) and supercavitaiton (using a two-teeth rotor), that were generated inside the RGHC device. The high-speed camera revealed that behind every gap between the tips of the teeth of the opposing serrated rotor and stator a developed unsteady form of cavitation was accompanied by bubble cloud shedding and collapse. Moreover, when the two-teeth rotor was spun, almost the entire section behind every tip of both teeth was engulfed within a vapour cavity (Fig. 5D).

These two types of hydrodynamic cavitation generated inside the RGHC device were further tested for their antimicrobial potential against the high titers of bacteria *B. subtilis*. Unsteady developed cavitation generated inside the RGHC had a weak impact on the viability of *B. subtilis* and only slowly reduced its viable count (μ of -0.83). However, when supercavitation was applied, the viable count of *B. subtilis* was reduced by 2.3 logs (μ of -5.22). Therefore, for the same treatment times (1 h), the destruction of bacteria *B. subtilis* was 5.8 times more efficient for the supercavitation in comparison to the unsteady developed cavitation (0.4 logs reduction). Similar trends were repeated for the low initial bacterial titers. Even though for supercavitation larger disturbances in pressure are uncommon [8] it has already been successfully applied for the destruction of the troublesome bacteria *L. pneumophila* [28]. The main mechanism by which supercavitation disrupts bacterial cells is currently unknown, however it might be the result of multiple simultaneous effects such as instant pressure decrease at the entrance of supercavity (transition from liquid to vapour phase) [29] and the generation of very high shear forces (shear rate of $2.6 \cdot 10^4\ s^{-1}$; which is circumferential velocity/1 mm gap height between rotor and stator). In

fact, according to literature, high shear stress can cause extensive cell damage ending with cell hemolysis [45].

Supercavitation treatment was found to reduce the viability of all the major classes of microorganisms present in the RW samples which were isolated from a paper producing plant. This was especially evident for the anaerobic sulphate reducing bacteria (μ of -9.70) and for the yeasts (μ of -9.00) for which a strong reduction of around 4 logs was achieved. A strong reduction of 3 logs was also observed for the aerobic bacteria (μ of -6.26). Interestingly, even bacterial spores which are highly resistant to mechanical and physical stresses were reduced by 1.3 logs (μ of -2.9). The destruction of these groups of microorganisms is particularly important for the paper producing industry especially when an enclosed water recycle system is employed [34,46,47].

Supercavitation treatment decreased COD and increased the dissolved oxygen content and redox potential (up to 77 %) in the RW samples. Decrease in COD indicates that supercavitation significantly contributed to the degradation of organic contaminants. This could be due to the formation of $^{\bullet}$OH radicals which act as oxidants for organic molecules [48]. As described in chapter 3.1, supercavitation, which is formed on the presented rotor, also consists of the shedding part where due to individual bubble collapses radical formation is possible. To determine if the COD removal is caused by radicals a scavenger such as methanol could be added to the sample. At similar pH values (pH of 7) to that of the RW samples (pH of 7.6), the $^{\bullet}$OH radicals exhibit a strong redox potential of +2.31 V as measured by the normal hydrogen electrode [49]. Therefore, the formation of $^{\bullet}$OH radicals and the increase in dissolved oxygen level consequently elevated the redox potential of water [50]. When water jets in hydrodynamic cavitation systems travel through

air, they draw substantial quantities of air and the high pressures which are generated during cavitation can dissolve the air into the water [51].

Supercavitation reduced the sediments and the insoluble materials and generally intensified all the SAC colour values in the RW samples. Because bacteria represent a significant part of the sediment, the destruction of cells by supercavitation could cause a reduction in insoluble sediments. Furthermore, Poyato et al. [52] showed that cavitation can break insoluble particles into smaller sized fragments which are termed as total suspended solids (TSS), and these are small enough not to settle down and will indefinitely remain suspended in the solution which isn't subjected to any form of motion. Colour pollutants in water samples are problematic because they limit the amount of light entering into the water consequently having an inhibiting effect on photosynthesizing organisms and phytoremediation [53]. The increase in colour by supercavitation is, however, not alarming, because it did not exceed the concentration limits of emission into water determined by the European Norm EN ISO 7887, which are 7 m^{-1} for 436 nm (yellow), 5 m^{-1} for 525 nm (red), and 3 m^{-1} for 620 nm (blue) [54]. In accordance with our results, Lorimer et al. [55] observed that ultrasonic cavitation reduces the colour removal capability of the electrolytic treatment by disintegrating solid particles present in the samples. The disintegration of larger insoluble particles into many smaller sized particles can contribute to the intensification of colour values.

Lastly, in comparison to the RW samples, supercavitation had a significantly smaller impact on the destruction of microorganisms and on the reduction of COD in the CRW samples. One clear difference between these two types of samples was that only the CRW samples were intensely

foaming during cavitation. Due to the foaming the cavitation could not result in one stable supercavity, instead large number of smaller cavitation bubbles were formed, which might have reduced the chance of bacteria entering into the area of low pressure. Additionally, the higher amount of smaller bubbles could lead to the cushioning effect which decreases the intensity of bubble collapses and amount of formed radicals and results in lower COD removal.

The economic analysis showed that for a similar initial bacterial titer, our RGHC, which generated supercavitation, spent 4 times less electrical energy for the reduction of bacteria *B. subtilis* (67.2 kWh/m^3/order) in comparison to the Venturi device which was used for the reduction of *E. coli* (268.6 kWh/m^3/order) and was assembled by Arrojo et al. [43]. Moreover, it has to be mentioned that in our experiments the highly resistant Gram-positive *B. subtilis* was used (wall thickness of 30 nm [56]; may bear a turgor pressure of 2.6 MPa [57]) whereas in the experiments performed by Arrojo et al. [43] the more susceptible Gram negative *E. coli* was adopted (wall thickness of 2-4 nm [58,59]; may bear a turgor pressure of 29 kPa [60]). Furthermore, the efficiency of the RGHC was especially high for the anaerobic sulphate reducing bacteria and for yeasts isolated form the RW samples (3.6 €/m^3 - 3.9 €/m^3). This device possesses a number of advantages over previous designs. For example, the RGHC can generate greater shear forces (during supercavitation shear rate was $2.6 \cdot 10^4$ s^{-1}; and Rotational Reynolds number was $1.1 \cdot 10^6$ [61]) which are caused by the rotation of the rotor and the liquid that is located between the rotor and the stator.

5. Conclusions

This study evaluates the efficiency of a lab-scale rotation generator of hydrodynamic cavitation for the treatment of a process water isolated from an enclosed water recycle system of a paper producing plant. Two set-ups capable of generating different type of cavitation, namely developed cavitation and supercavitation, were tested. Our results showed that supercavitation was more efficient for the destruction of *B. subtilis,* Gram positive bacteria problematic in paper mill production plants. The results were evaluated in terms of chemical, physical and microbiological characterisation. Using the supercavitation set-up we were able to destroy 2.3 logs of *B. subtilis*, 4.2 logs of anaerobic sulphate reducing bacteria, 4 logs of yeast, 3 logs of aerobic bacteria and 1.3 logs of bacterial spores. In terms of chemical characterisation of samples, we achieved 22 % COD reduction, a 77 % increase in redox potential and a 27 % increase in dissolved oxygen levels. Evaluation of physical characterisation of treated samples showed that sediment portion was reduced by 50 % and the insoluble portion by 67 %. When the achieved results are compared to different cavitation set-ups, it can be deduced that rotation cavitation generator of supercavitation is economically more feasible than for example a Venturi device.

Based on the achieved results we plan to investigate the efficiency of the rotation generator of hydrodynamic cavitation on a pilot scale integrated into the enclosed water recycle system of a paper plant.

Acknowledgments

The authors would like to thank the Slovenia's Smart Specialisation Strategy for funding the Research, development and innovation project (RDI) Cel.Cycle: »Potential of biomass for development of advanced materials and bio-based products« (contract number: OP20.00365), which is cofinanced by the Ministry of Education, Science and Sport of the Republic of Slovenia and the European Union as part of the European Regional Development Fund 2016 – 2020; and the Slovenian Research Agency for funding the core research No. P2-0401. We thank the paper company Vipap Videm Krško for their cooperation and support. Mathematical and grammatical help was provided by Professors Franc Kosel and Bernarda Kosel.

References:

[1] O.M. Väisänen, E.L. Nurmiaho-Lassila, S.A. Marmo, M.S. Salkinoja-Salonen, Structure and composition of biological slimes on paper and board machines., Appl. Environ. Microbiol. 60 (1994) 641–53. http://www.ncbi.nlm.nih.gov/pubmed/16349191 (accessed March 28, 2019).

[2] C. Kanto Öqvist, J. Kurola, J. Pakarinen, J. Ekman, S. Ikävalko, J. Simell, M. Salkinoja-Salonen, Prokaryotic microbiota of recycled paper mills with low or zero effluent, J. Ind. Microbiol. Biotechnol. 35 (2008) 1165–1173. doi:10.1007/s10295-008-0396-8.

[3] M. Kolari, J. Nuutinen, F.A. Rainey, M.S. Salkinoja-Salonen, Colored moderately thermophilic bacteria in paper-machine biofilms, J. Ind. Microbiol. Biotechnol. 30 (2003) 225–238. doi:10.1007/s10295-003-0047-z.

[4] L. Mezule, S. Tsyfansky, V. Yakushevich, T. Juhna, A simple technique for water disinfection with hydrodynamic cavitation: Effect on survival of Escherichia coli, Desalination. 248 (2009) 152–159. doi:10.1016/j.desal.2008.05.051.

[5] E.R. Nestmann, E.G.-H. Lee, T.I. Matula, G.R. Douglas, J.C. Mueller, Mutagenicity of constituents identified in pulp and paper mill effluents using the Salmonella/mammalian-microsome assay, Mutat. Res. Toxicol. 79 (1980) 203–212. doi:10.1016/0165-1218(80)90067-1.

[6] European Commission, Decision commission of 7 June 2011 on establishing the ecological criteria for the award of the EU Ecolabel for copying and graphic paper, Off. J. Eur. Union. (2011) 1–24.

[7] M. Dular, T. Griessler-Bulc, I. Gutierrez-Aguirre, E. Heath, T. Kosjek, A. Krivograd Klemenčič, M. Oder, M. Petkovšek, N. Rački, M. Ravnikar, A. Šarc, B. Širok, M. Zupanc, M. Žitnik, B. Kompare, Use of hydrodynamic cavitation in (waste)water treatment, Ultrason. Sonochem. 29 (2016) 577–588. doi:10.1016/j.ultsonch.2015.10.010.

[8] J.P. Franc, J.M. Michel, Fundamentals of Cavitation, Kluwer Academic Publishers, 2004.

[9] J.D. Seymour, R.B. Gupta, Oxidation of Aqueous Pollutants Using Ultrasound: Salt-Induced Enhancement, Ind. Eng. Chem. Res. 36 (1997) 3453–3457. doi:10.1021/ie970069o.

[10] A.B. Pandit, P.R. Gogate, S. Mujumdar, Ultrasonic degradation of 2:4:6 trichlorophenol in presence of TiO2 catalyst, Ultrason. Sonochem. 8 (2001) 227–231. doi:10.1016/S1350-4177(01)00081-5.

[11] N.S.M. Yusof, B. Babgi, Y. Alghamdi, M. Aksu, J. Madhavan, M. Ashokkumar, Physical and chemical effects of acoustic cavitation in selected ultrasonic cleaning applications, Ultrason. Sonochem. 29 (2016) 568–576. doi:10.1016/J.ULTSONCH.2015.06.013.

[12] N. Vyas, K. Manmi, Q. Wang, A.J. Jadhav, M. Barigou, R.L. Sammons, S.A. Kuehne, A.D. Walmsley, Which Parameters Affect Biofilm Removal with Acoustic Cavitation? A Review, Ultrasound Med. Biol. 45 (2019) 1044–1055. doi:10.1016/J.ULTRASMEDBIO.2019.01.002.

[13] X. Li, T. Zhu, K. Zhang, L. Lv, T. Chai, Y. Shen, Y. Wang, M. You, Y. Xie, Effect of the sequence ultrasonic operation on anaerobic degradation of sewage sludge, Int. Biodeterior. Biodegradation. 112 (2016) 66–71. doi:10.1016/J.IBIOD.2016.05.006.

[14] K.S. Suslick, M.M. Mdleleni, J.T. Ries, Chemistry induced by hydrodynamic cavitation, J. Am. Chem. Soc. 119 (1997) 9303–9304. doi:10.1021/ja972171i.

[15] K.R. Morison, C.A. Hutchinson, Limitations of the Weissler reaction as a model reaction for measuring the efficiency of hydrodynamic cavitation, Ultrason. Sonochem. 16 (2009) 176–183. doi:10.1016/j.ultsonch.2008.07.001.

[16] N. Arul Dhas, A. Gedanken, Sonochemical Synthesis of Molybdenum Oxide- and Molybdenum Carbide-Silica Nanocomposites, Chem. Mater. 9 (1997) 3144–3154. doi:10.1021/cm9704488.

[17] S. Drakopoulou, S. Terzakis, M.S. Fountoulakis, D. Mantzavinos, T. Manios, Ultrasound-induced inactivation of gram-negative and gram-positive bacteria in secondary treated municipal wastewater, Ultrason. Sonochem. 16 (2009) 629–634. doi:10.1016/j.ultsonch.2008.11.011.

[18] J. Zhang, J. Du, B. Han, Z. Liu, T. Jiang, Z. Zhang, Sonochemical Formation of Single-Crystalline Gold Nanobelts, Angew. Chemie Int. Ed. 45 (2006) 1116–1119. doi:10.1002/anie.200503762.

[19] C.A. Lopes, V. Jofre, M.P. Sangorrin, Spoilage yeasts in Patagonian winemaking: molecular and physiological features of Pichia guilliermondii indigenous isolates, Rev. Argentina Microbiol. 41 (2009) 177–184. http://www.scielo.org.ar/scielo.php?script=sci_arttext&pid=S0325-

75412009000300010&nrm=iso.

[20] N.S.M. Yusof, M. Ashokkumar, Ultrasound-induced formation of high and low viscoelastic nanostructures of micelles, Soft Matter. 9 (2013) 1997. doi:10.1039/c2sm27423j.

[21] P.S. Kumar, A.B. Pandit, Modeling Hydrodynamic Cavitation, Chem. Eng. Technol. 22 (1999) 1017–1027. doi:10.1002/(SICI)1521-4125(199912)22:12<1017::AID-CEAT1017>3.0.CO;2-L.

[22] A.G. Chakinala, P.R. Gogate, R. Chand, D.H. Bremner, R. Molina, A.E. Burgess, Intensification of oxidation capacity using chloroalkanes as additives in hydrodynamic and acoustic cavitation reactors, Ultrason. Sonochem. 15 (2008) 164–170. doi:10.1016/j.ultsonch.2007.02.008.

[23] P.R. Gogate, A.B. Pandit, A review of imperative technologies for wastewater treatment I: oxidation technologies at ambient conditions, Adv. Environ. Res. 8 (2004) 501–551. doi:10.1016/S1093-0191(03)00032-7.

[24] S. Arrojo, Y. Benito, A theoretical study of hydrodynamic cavitation, Ultrason. Sonochem. 15 (2008) 203–211. doi:10.1016/j.ultsonch.2007.03.007.

[25] J.-P. Franc, Physics and Control of Cavitation, (2006).

[26] C. von Eiff, J. Overbeck, G. Haupt, M. Herrmann, S. Winckler, K.D. Richter, G. Peters, H.U. Spiegel, Bactericidal effect of extracorporeal shock waves on Staphylococcus aureus., J. Med. Microbiol. 49 (2000) 709–12. doi:10.1099/0022-1317-49-8-709.

[27] P. Riesz, T. Kondo, Free radical formation induced by ultrasound and its biological

implications., Free Radic. Biol. Med. 13 (1992) 247–70.

[28] A. Šarc, M. Oder, M. Dular, Can rapid pressure decrease induced by supercavitation efficiently eradicate Legionella pneumophila bacteria?, Desalin. Water Treat. 57 (2016) 2184–2194. doi:10.1080/19443994.2014.979240.

[29] R.A. Gottlieb, S. Adachi, Nitrogen cavitation for cell disruption to obtain mitochondria from cultured cells., Methods Enzymol. 322 (2000) 213–21. http://www.ncbi.nlm.nih.gov/pubmed/10914019 (accessed July 26, 2017).

[30] M. Petkovšek, M. Mlakar, M. Levstek, M. Stražar, B. Širok, M. Dular, A novel rotation generator of hydrodynamic cavitation for waste-activated sludge disintegration, Ultrason. Sonochem. 26 (2015) 408–414. doi:10.1016/j.ultsonch.2015.01.006.

[31] E.J. Hayhurst, L. Kailas, J.K. Hobbs, S.J. Foster, Cell wall peptidoglycan architecture in Bacillus subtilis., Proc. Natl. Acad. Sci. U. S. A. 105 (2008) 14603–8. doi:10.1073/pnas.0804138105.

[32] M. Rättö, M. Siika-aho, J. Buchert, A. Valkeajävi, L. Viikari, Enzymatic hydrolosis of isolated and fibre-bound galactoglucomannans from pine-wood and pine kraft pulp, Appl. Microbiol. Biotechnol. 40 (1993) 449–454. doi:10.1007/BF00170409.

[33] O.M. Väisänen, A. Weber, A. Bennasar, F.A. Rainey, H.J. Busse, M.S. Salkinoja-Salonen, Microbial communities of printing paper machines., J. Appl. Microbiol. 84 (1998) 1069–84.

[34] O. Priha, K. Hallamaa, M. Saarela, L. Raaska, Detection of Bacillus cereus group bacteria from cardboard and paper with real-time PCR, J. Ind. Microbiol. Biotechnol. 31 (2004)

161–169. doi:10.1007/s10295-004-0125-x.

[35] ISO, ISO 15874-3:2003 - Plastics piping systems for hot and cold water installations -- Polypropylene (PP) -- Part 3: Fittings, (2003).

[36] M. Zupanc, T. Kosjek, M. Petkovšek, M. Dular, B. Kompare, B. Širok, Ž. Blaženka, E. Heath, Removal of pharmaceuticals from wastewater by biological processes, hydrodynamic cavitation and UV treatment, Ultrason. Sonochem. 20 (2013) 1104–1112. doi:10.1016/j.ultsonch.2012.12.003.

[37] ES ISO 6611, Milk and milk products - Enumeration of colony-forming units of yeasts and/or moulds - Colony-count technique at 25 °C, (2012).

[38] R. Maier, Bacterial Growth, in: R. Maier, I. Pepper, C. Gerba (Eds.), Environ. Microbiol., 397th ed., Academic press, 2009: pp. 37–40.

[39] DIN 38409-2, German standard methods for the examination of water, waste water and sludge; parameters characterizing effects and substances (group H); determination of filterable matter and the residue on ignition (H 2)9-2, (1980).

[40] SIST ISO 11923, Water quality - Determination of suspended solids by filtration through glass-fibre filters, 020654 (1998).

[41] ISO 7887, Water quality - Examination and determination of colour, (1996).

[42] A. Šarc, J. Kosel, D. Stopar, M. Oder, M. Dular, Removal of bacteria Legionella pneumophila, Escherichia coli, and Bacillus subtilis by (super)cavitation, Ultrason. Sonochem. 42 (2018). doi:10.1016/j.ultsonch.2017.11.004.

[43] S. Arrojo, Y. Benito, A. Martínez Tarifa, A parametrical study of disinfection with

hydrodynamic cavitation, Ultrason. Sonochem. 15 (2008) 903–908. doi:10.1016/j.ultsonch.2007.11.001.

[44] J.R. Bolton, K.G. Bircher, W. Tumas, C.A. Tolman, Figures-of-merit for the technical development and application of advanced oxidation technologies for both electric- and solar-driven systems (IUPAC Technical Report), Pure Appl. Chem. 73 (2001) 627–637. doi:10.1351/pac200173040627.

[45] L.B. Leverett, J.D. Hellums, C.P. Alfrey, E.C. Lynch, Red Blood Cell Damage by Shear Stress, Biophys. J. 12 (1972) 257–273. doi:10.1016/S0006-3495(72)86085-5.

[46] M. Kolari, Paper machine microbiology, in: Handb. Papermak. Chem. Chapt 6, Finnish Paper Engineers' Association, Helsinki, 2007: pp. 181–198.

[47] C. Kanto Öqvist, J. Kurola, J. Pakarinen, J. Ekman, S. Ikävalko, J. Simell, M. Salkinoja-Salonen, Prokaryotic microbiota of recycled paper mills with low or zero effluent, J. Ind. Microbiol. Biotechnol. 35 (2008) 1165–1173. doi:10.1007/s10295-008-0396-8.

[48] M. Badve, P. Gogate, A. Pandit, L. Csoka, Hydrodynamic cavitation as a novel approach for wastewater treatment in wood finishing industry, Sep. Purif. Technol. 106 (2013) 15–21. doi:10.1016/j.seppur.2012.12.029.

[49] M. Topaz, V. Shuster, E.I. Assia, D. Meyerstein, N. Meyerstein, D. Mazor, A. Gedanken, Acoustic cavitation in phacoemulsification and the role of antioxidants, Ultrasound Med. Biol. 31 (2005) 1123–1129. doi:10.1016/J.ULTRASMEDBIO.2005.02.016.

[50] N.P. Cheremisinoff, Handbook of Solid Waste Management and Waste Minimization Technologies, Butterworth-Heinemann, 2003.

[51] Global Advantech Limited, Cavitation Stripping Gases from Liquids and Oxygenation and Biological Control, Technol. Data Sheet TDS806. (2012). www.globaladvantech.com.

[52] J. Poyato, J.L. Pérez-Rodríguez, V. Ramírez-Valle, A. Lerf, F.E. Wagner, Sonication induced redox reactions of the Ojén (Andalucía, Spain) vermiculite, Ultrason. Sonochem. 16 (2009) 570–576. doi:10.1016/J.ULTSONCH.2008.12.009.

[53] Č. Novotný, K. Svobodová, O. Benada, O. Kofroňová, A. Heissenberger, W. Fuchs, Potential of combined fungal and bacterial treatment for color removal in textile wastewater, Bioresour. Technol. 102 (2011) 879–888. doi:10.1016/J.BIORTECH.2010.09.014.

[54] F. Çiner, Ö. Gökkuş, Treatability of dye solutions containing disperse dyes by fenton and fenton-solar light oxidation processes, Clean - Soil, Air, Water. 41 (2013) 80–85. doi:10.1002/clen.201000500.

[55] J.. Lorimer, T.. Mason, M. Plattes, S.. Phull, Dye effluent decolourisation using ultrasonically assisted electro-oxidation, Ultrason. Sonochem. 7 (2000) 237–242. doi:10.1016/S1350-4177(99)00045-0.

[56] M. Beeby, J.C. Gumbart, B. Roux, G.J. Jensen, Architecture and assembly of the Gram-positive cell wall, Mol. Microbiol. 88 (2013) 664–672. doi:10.1111/mmi.12203.

[57] J.J. Thwaites, U.C. Surana, Mechanical properties of Bacillus subtilis cell walls: Effects of removing residual culture medium, J. Bacteriol. 173 (1991) 197–203. doi:10.1128/jb.173.1.197-203.1991.

[58] R.D. Turner, A.F. Hurd, A. Cadby, J.K. Hobbs, S.J. Foster, Cell wall elongation mode in

Gram-negative bacteria is determined by peptidoglycan architecture., Nat. Commun. 4 (2013) 1496. doi:10.1038/ncomms2503.

[59] B. Glauner, J. V Höltje, U. Schwarz, The composition of the murein of Escherichia coli., J. Biol. Chem. 263 (1988) 10088–95.

[60] Y. Deng, M. Sun, J.W. Shaevitz, Direct measurement of cell wall stress stiffening and turgor pressure in live bacterial cells, Phys. Rev. Lett. 107 (2011) 7–10. doi:10.1103/PhysRevLett.107.158101.

[61] M. Farzaneh-Gord, A. Vazifedoost, A.B. Khoshnevis, Numerical study of flow in a rotor-stator system with inward throughflow, Arch. Mech. 62 (2010) 195–214. doi:10.24423/AOM.326.

Declaration of interests

☒ The authors declare that they have no known competing financial interests or personal relationships that could have appeared to influence the work reported in this paper.

☐The authors declare the following financial interests/personal relationships which may be considered as potential competing interests: